Region-specific Microtubule Transport in Motile Cells

Anne-Marie C. Yvon* and Patricia Wadsworth‡

*Molecular and Cellular Biology Program and ‡Department of Biology, University of Massachusetts, Amherst, Massachusetts 01003

Abstract. Photoactivation and photobleaching of fluorescence were used to determine the mechanism by which microtubules (MTs) are remodeled in PtK2 cells during fibroblast-like motility in response to hepatocyte growth factor (HGF). The data show that MTs are transported during cell motility in an actomyosin-dependent manner, and that the direction of transport depends on the dominant force in the region examined. MTs in the leading lamella move rearward relative to the substrate, as has been reported in newt cells (Waterman-Storer, C.M., and E.D. Salmon. 1997. *J. Cell Biol.* 139:417–434), whereas MTs in the cell body and in the retraction tail move forward, in the direction of cell locomotion. In the transition zone between the peripheral lamella and the cell body, a subset of MTs remains stationary with respect to the substrate, whereas neighboring MTs are transported either forward, with the cell body, or rearward, with actomyosin retrograde flow. In addition to transport, the photoactivated region frequently broadens, indicating that individual marked MTs are moved either at different rates or in different directions. Mark broadening is also observed in nonmotile cells, indicating that this aspect of transport is independent of cell locomotion. Quantitative measurements of the dissipation of photoactivated fluorescence show that, compared with MTs in control nonmotile cells, MT turnover is increased twofold in the lamella of HGF-treated cells but unchanged in the retraction tail, demonstrating that microtubule turnover is regionally regulated.

Key words: microtubules • cell motility • photoactivation • transport • turnover

Introduction

A notable feature of the microtubule (MT)[1] cytoskeleton is its capacity for rapid reorganization. Perhaps the most dramatic example of MT rearrangement occurs at the entry into mitosis, when the interphase cytoskeleton is disassembled and the mitotic spindle is assembled. Upon completion of mitosis, the interphase array is reestablished. During cell motility, the MT array must also be remodeled continually as MTs populate the advancing lamella and vacate retracting regions. Cell motility results from a cycle of protrusion at the leading edge, adhesion, and contraction at the cell rear, events that require dynamic actin assemblies and actomyosin-generated contractile forces (Harris, 1994; Mitchison and Cramer, 1996). Small, highly motile cells move directionally in the absence of MTs (Euteneuer and Schliwa, 1984), whereas MT disassembly in larger cells results in a loss of polarity and cessation of motility (Vasiliev, 1991). In some cell types, stable MTs are oriented in the direction of migration, consistent with a role for MTs in the establishment and maintenance of cell polarity (Gundersen and Bulinski, 1988). MT dynamic turnover must also be important for efficient locomotion, as the suppression of MT dynamic instability (the stochastic switching of MT ends between phases of growth and shortening [Mitchison and Kirschner, 1984]) with low doses of nocodazole or vinblastine reduces directional migration in wound edge cells and in migrating nerve growth cones (Liao et al., 1995; Tanaka et al., 1995). Recent work indicates that dynamic MTs target sites of cell–substrate adhesion and contribute to the turnover of adhesion sites. Disruption of MTs also alters cell contractility, indicating physical and/or biochemical interaction(s) between the MT and microfilament cytoskeletons (Danowski, 1989).

Two recent studies have mapped the mechanical forces exerted on the substrate by locomoting fibroblast cells (Galbraith and Sheetz, 1997; Pelham and Wang, 1999). Both reports document rearward forces in the anterior of the cell, forward forces in the posterior, and a region in which the direction of forces changes, under the nucleus (Galbraith and Sheetz, 1997) or in a region anterior to the nucleus (Pelham and Wang, 1999). To test the hypothesis that forces generated by cell locomotion contribute to MT remodeling, we have used photobleaching and photoacti-

Address correspondence to Patricia Wadsworth, University of Massachusetts, 221 Morrill Science Center, Amherst, MA 01003. Tel.: (413) 545-4877. Fax: (413) 545-3243. E-mail: patw@bio.umass.edu

[1]*Abbreviations used in this paper:* BDM, 2,3-butane-dione-monoxime; HGF, hepatocyte growth factor; MT, microtubule.

vation to mark MTs in PtK2 cells undergoing fibroblast-like motility in response to hepatocyte growth factor (HGF). Our results show that MTs are moved in the direction of the dominant actomyosin–generated force: retrograde flow from the front or contraction from the rear. Our results support the Pelham and Wang (1999) study, given that we see MTs moved in both directions in the region ahead of the nucleus, but never in the perinuclear region itself. Our data further show that internal cellular components are moved in a pattern corresponding with that of the forces exerted by the cell on the substrate. We have also measured the turnover half time for the population of MTs in motile and non-motile cells and have found that turnover is increased in the lamella of HGF-treated cells and unchanged in the retraction tail, compared with controls. We conclude that MT transport is likely to play an important and previously unrecognized role in the reorganization of MTs in diverse cells.

Materials and Methods

All materials for cell culture were obtained from GIBCO BRL, with the exception of fetal calf serum, which was obtained from Atlanta Biologicals. PtK2 cells were the kind gift of Dr. Barbara Danowski (Union College, Schenectady, NY). Unless otherwise noted, all other chemicals were obtained from Sigma-Aldrich.

Preparation of Labeled Tubulins

Tubulin labeling was performed using the high pH method as described (Desai and Mitchinson, 1998). In brief, phosphocellulose-purified porcine tubulin (Sloboda et al., 1976) was assembled, centrifuged through a 60% glycerol cushion, pH 8.6, and MTs were resuspended and incubated with 0.01 M 5,6-COOH succinimidyl ester of rhodamine (Molecular Probes) or with 2.5 nM C2CF in DMSO (the kind gift of Drs. Arshad Desai and Timothy Mitchison, Harvard University, Cambridge, MA). The conjugated MTs were collected by centrifugation through a 60% glycerol cushion, pH 6.8, resuspended in injection buffer (50 mM glutamate and 0.5 mM $MgCl_2$, pH 7.0), and disassembled on ice for 30 min. The protein was centrifuged and the supernatant was retained, carried through another cycle of temperature-dependent assembly and disassembly, and stored at −80°C in small aliquots. For labeling with C2CF, the entire procedure was carried out under a safelight.

Cell Culture and Microinjection

PtK2 cells were grown with 5% CO_2 at 37°C in 90% MEM supplemented with 1.0 mM sodium pyruvate, 10% fetal calf serum and antibiotics. For use in experiments, cells were plated on etched glass coverslips (Bellco Glass Co.) 1–2 d before use. HGF-conditioned medium was prepared from MRC5 cells, which secrete the growth factor (Stoker et al., 1987). Growth medium was replaced with HGF-conditioned medium ~24 h before experiments were to be performed.

Microinjection was performed exactly as described previously (Yvon and Wadsworth, 1997). For photobleaching experiments, rhodamine tubulin was microinjected at a needle concentration of 1.2 mg/ml; for coinjection of C2CF and rhodamine tubulins, the needle concentrations were 1.9 and 0.8 mg/ml, respectively. After injection, the cells were returned to a 37°C incubator for at least 90 min to allow incorporation of the labeled tubulin into MTs. To prevent photodamage, an oxygen scavenging enzyme system, EC Oxyrase (Oxyrase Inc.), was added to the medium at a concentration of 0.3 U/ml before observation of live cells (Waterman-Storer et al., 1993). For some experiments, a 5 M stock solution of 2,3-butanedione-monoxime (BDM) in methanol was added to the medium at a final concentration of 20 mM.

Cell Staining

Immunofluorescence localization of MTs was performed exactly as described previously (Yvon and Wadsworth, 1997). Rhodamine phalloidin (Molecular Probes) was used to visualize F-actin. 10 μl of the supplied 6.6 μM solution was dried down and resuspended in 100 μl of PBS containing 0.1% Tween 20 and 0.02% azide. Cells were incubated in phalloidin for 20 min at room temperature and rinsed thoroughly with PBS containing 0.1% Tween 20 and 0.02% azide. For immunofluorescence localization of vinculin and myosin, cells were fixed in 3.7% formaldehyde and incubated either in a monoclonal antivinculin antibody (clone VIN 11-5, 1:50 dilution; Sigma-Aldrich), followed by incubation in Cy3-conjugated goat anti–mouse secondary antibodies (1:200 dilution; Jackson ImmunoResearch Laboratories), or in a polyclonal anti–human blood platelet myosin antibody (1:25 dilution; Biomedical Technologies, Inc.), followed by incubation in fluorescein-conjugated goat anti–rabbit secondary antibodies (1:200 dilution; Organon Teknika). Stained coverslips were mounted in Vectashield (Vector Laboratories), and sealed with clear nail polish.

Image Collection

Fluorescent MTs in injected cells were imaged using a confocal microscope equipped with a krypton/argon ion laser scanning head (model MRC-600; Bio-Rad Laboratories) mounted on a Nikon Diaphot 200 with a rotating stage, a stepper motor, and a 60× 1.4 numerical aperture objective lens. Caged tubulin was photoactivated by a 4-s exposure to unattenuated 360-nm light, using a shuttered mercury arc epiilluminator with a DAPI fluorescence filter cube and a 25 μm × 3 mm slit (Coherent-Ealing) on a slider in a conjugate image plane. For all experiments, the scan head was operated with the pinholes fully open and the laser at 0.3% intensity; a single, unaveraged image was taken using the slow scanning laser mode. Simultaneous images of the entire MT array and the photoactivated MTs were collected, beginning immediately after photoactivation. To demonstrate that MTs through the entire cell thickness were photoactivated, scanning in the z-axis was performed on selected cells. Photoactivation of MTs in the retraction tail was performed on a Nikon Eclipse TE300 equipped with a rotating stage, a 100× 1.3 numerical aperture objective lens, and dual filter wheels. Caged tubulin was photoactivated as described above except that the slit was mounted in a wheel rather than on a slider. Metamorph® imaging software (Universal Imaging) and a Princeton Instruments MicroMAX™ interline transfer CCD camera were used to collect paired images of the entire rhodamine-labeled array and the photoactivated C2CF-labeled region at 2-min intervals for a total of 1 h.

For photobleaching experiments, the previously described confocal microscope was used. The laser was switched to the fast scanning mode at 100% power to bleach a selected region; subsequent images in the rhodamine channel were collected at intervals ranging from 15 to 45 s for a total of 3–5 min. The selected region was within 15 μm of the cell membrane, and was in the leading edge of motile cells and in the "free" edge (i.e., not in contact with neighboring cells) of nonmotile cells. For fixed cells, a Z-series of 0.5 μm-steps for a total of 7–8 μm was collected. Phase images were collected on the Nikon Eclipse TE300 using a 60× 1.4 numerical aperture lens. Images were printed using Adobe Photoshop® software (Adobe Systems) running on a Power Macintosh G3 with an Epson Stylus 850N printer.

Data Analysis

For calculating the rates of nuclear migration, lamellar extension, tail retraction, movement of the photoactivated mark, retrograde movement of parallel MTs, or photobleached marks on peripheral MTs, the Measure Distance function of Metamorph® imaging software was used with a dynamic data exchange connection to an Excel spreadsheet (Microsoft Corporation). For measurement of lamellar extension and most photoactivated marks (measured from the center, width-wise, of the fluorescent bar), two to four different locations along the length were measured and averaged. Photoactivated tail MTs were measured from the center of the mark; nuclear position was measured from the center of the leading edge of the nucleus; tail position was measured from the tip of the tail. The rearward movement of parallel MTs in the peripheral lamella was uniform, and was therefore measured from one point along the length; photobleached marks were measured from whichever edge of the mark was clearer throughout the sequence. Distance between the initial point and the final point was reported by Metamorph® and divided by the elapsed time to calculate rates.

Turnover of the MT array was also analyzed using Metamorph®. Care was taken to use image sequences in which the focal plane was constant and the initial fluorescence was not saturated. For quantification of turnover in untreated cells, photoactivation was performed in the central lamellar region; in HGF-treated cells, photoactivation was performed toward the rear of the peripheral lamella, just before the transition zone, and at the approximate center of the tail. A box was drawn around the photoactivated region on the first image of the stack, using the Region

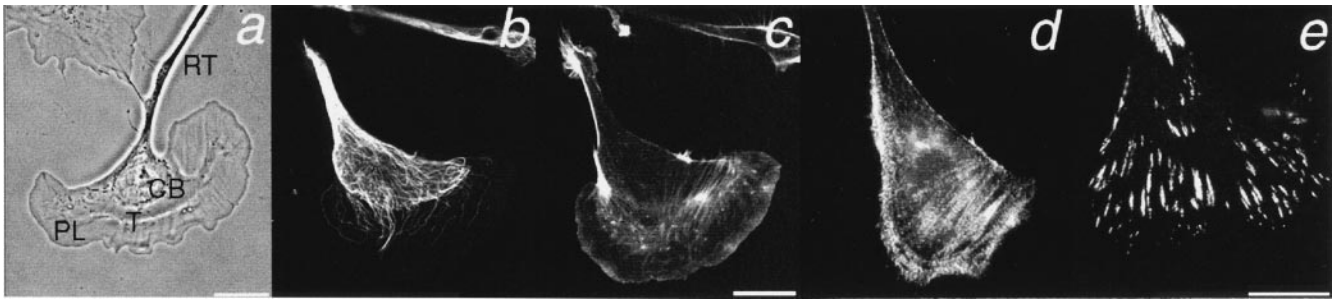

Figure 1. Cytoskeletal organization in HGF-treated PtK2 cells. Phase image (a) showing the general appearance and defined regions of the cell; fluorescence images showing the localization of MTs (b), F-actin (c), myosin (d) and vinculin (e). b and c are the same cell, all other panels show different cells. PL, peripheral lamella; T, transition zone; CB, cell body; RT, retraction tail. b and c, and d and e share marker bars. Bars, 20 μm.

Tools. The dimensions of the box were then adjusted with respect to the last image of the stack, to ensure that the photoactivated region was within the box for the entire sequence, even after its translocation. A second box with exactly the same dimensions as the first box was also placed on the images in an analogous region of the cell, containing no photoactivated MTs, to serve as a background measurement. The Threshold function was used to designate pixels to be measured, and the integrated pixel intensity was measured in both boxes for each image. The background intensity was subtracted and the initial time point was assigned a value of 100. Subsequent intensities were calculated as a percentage of the initial measurement. Several cells were measured and the values for each time point were averaged. Percent fluorescence (± SD) versus time, in minutes, was plotted using Origin® analytical software (Microcal Software, Inc.) and fitted to a single exponential decay.

Results

Morphology and Motile Characteristics of HGF-treated PtK2 Cells

Experiments were performed to test the hypothesis that MT transport contributes to reorganization of the MT array during cell motility (Waterman-Storer and Salmon, 1999). PtK cells treated with HGF disassemble cell–cell junctions and move in a fibroblast-like fashion, characterized by discontinuous phases of lamellar protrusion followed by nuclear advancement and tail retraction (see Fig. 3 c). The average rate of locomotion of HGF-treated cells, during the phase of nuclear advancement, is 0.7 μm/min.

MT transport was examined in different regions of HGF-treated cells, as defined in Fig. 1. Because MT behavior was the same in the regions typically designated as the lamella and lamellipodium (Cramer et al., 1997), they will be referred to collectively as the peripheral lamella (Lin and Forscher, 1993). The peripheral lamella is characterized by a sparse MT array (Fig. 1 b) and an actomyosin meshwork that is especially dense at the extreme cell periphery (Fig. 1, c and d). The cell body is defined as the region consisting of the nucleus and bulk cytoplasm. It has a dense MT array (Fig. 1 b), little F-actin (Fig. 1 c), and is substantially thicker in the z-axis than the peripheral lamella (7–9 vs. 1–2 μm). In most HGF-treated cells, though not all, there is a very clear boundary between the peripheral lamella and the cell body; this will be referred to as the transition zone (Fig. 1 a). The retraction tail extends from the cell body at the posterior of the cell and can be tens of microns long. The majority of focal contacts are located throughout the peripheral lamella and along the edges of the retraction tail, with fewer in the cell body (Fig. 1 e).

Retrograde Transport of MTs at the Periphery of Motile Cells

Previous results have shown that MTs at the leading edge of newt lung epithelial cells are swept rearward as a result of actomyosin-dependent retrograde flow (Waterman-Storer and Salmon, 1997). We performed photobleach marking experiments to determine whether MT retrograde transport is a general property of MTs at the periphery of motile cells, and if so, whether such movement differs when cells are actively extending a lamella and when they are not. The results show that there is retrograde transport of MTs in the peripheral lamella of HGF-treated cells (Fig. 2, a–c) and in that of control PtK2 cells (Fig. 2 d). For the purposes of this study, control cells are untreated, nonmotile PtK2 epithelial cells; retrograde transport was measured in the peripheral lamella of control cells at the edge of a patch and not in interior lamellae that contacted other cells. The rates of movement of individual MTs vary within and between cells, but the average rate is not statistically different for motile and nonmotile cells (Table I; Fig. 2, c and d). The rate of rearward movement is indistinguishable for MTs that are parallel or perpendicular to the leading edge (Table I), as previously noted (Waterman-Storer and Salmon, 1997), and is constant for MTs in both cells with lamella that are undergoing protrusion or those that are active but not extending. All photobleach marks were made within 15 μm of the leading edge; within this region, the rate of retro-

Table I. Average Movement Rates of the MTs, Nucleus, and Lamella in Different Regions of Motile Cells

Marked region cell type	Microtubules	Nucleus	Lamella
Peripheral lamella, untreated	0.18 ± 0.10 (8)	–	–
Parallel	0.20 ± 0.12	–	–
Perpendicular	0.15 ± 0.08	–	–
Peripheral lamella, HGF treated	0.21 ± 0.08 (12)	–	–
Parallel	0.23 ± 0.08	–	–
Perpendicular	0.20 ± 0.10	–	–
Cell body, HGF treated	0.48 ± 0.30 (7)	0.80 ± 0.32 (7)	0.26 ± 0.24 (5)

Rates are given in μm/min ± SD with the number of cells analyzed in parentheses. The nucleus was outside the field of view in experiments measuring the rearward movement of microtubules in the peripheral lamella and those measuring forward movement of microtubules in the retraction tail, and thus the rate of advancement could not be determined. In peripheral lamella experiments, the rate of lamellar extension was not determined because the time of observation (4 min for most cells) was too short for accurate measurement.

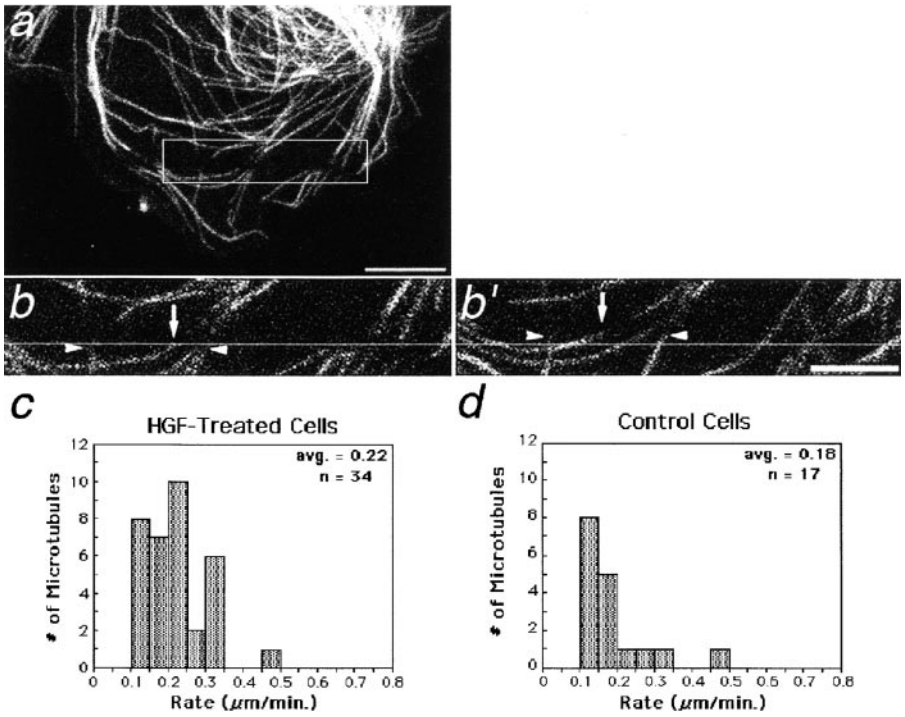

Figure 2. Rearward translocation of photobleached regions in the peripheral lamella of HGF-treated cells. Cell was microinjected with rhodamine-labeled tubulin. Outlined region in a is shown at higher magnification in b and b′; horizontal lines are provided as a reference. Image in b was collected immediately after laser photobleaching; that in b′ was collected 4 min after photobleaching. Arrowheads in b and b′ show retrograde movement of photobleached marks on MTs that are perpendicular to the leading edge; arrows show retrograde movement of a parallel MT. (The direction of motility is toward the bottom of the page.) The distributions of the rates of retrograde movement in HGF-treated and control cells are shown in c and d, respectively. Bars: (a) 10 μm; (b′) 5 μm.

grade MT movement was not dependent on the MTs' distance from the leading edge (data not shown).

In addition to rearward transport, the plus ends of MTs in this region undergo dynamic instability yet remain approximately the same distance from the plasma membrane, indicating that dynamic instability is biased toward growth, especially in actively extending regions (Waterman-Storer and Salmon, 1997; Wadsworth, 1999). Interestingly, during the period of observation (~4 min), ~25% of the MTs measured in HGF-treated cells did not undergo detectable rearward transport; in control cells, the fraction was closer to 50%.

MTs in the Cell Body of Motile Cells Move in the Direction of Cell Motility

Next, we used photoactivation of caged fluorescein (C2CF), conjugated to tubulin, to determine if MTs are transported in regions other than the peripheral lamella or if they are stationary with respect to the substrate as the cell advances. Alternatively, microtubules could behave nonuniformly. For example, there are two populations of F-actin in the cell body of migrating heart fibroblasts: a subset which advances with the cell body and one which remains stationary (Cramer et al., 1997). We found that photoactivated marks on MTs in the cell body of HGF-treated cells always move forward, in the direction of cell motility; an example of this behavior is shown in Fig. 3. Measurements of the rate of forward movement of photoactivated regions in the cell body and of nuclear motion in HGF-treated cells showed that the average rate of nuclear motion was greater than the average rate of the photoactivated mark movement (see Table I). As expected from the differences in these rates, the nucleus approached and, if observed for long enough, overtook the photoactivated bar (Fig. 3). Note that in HGF-treated cells, motility typi-

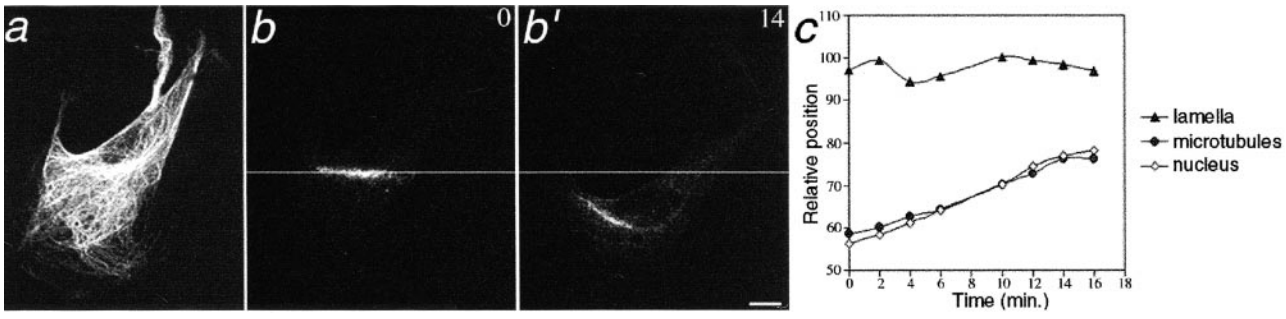

Figure 3. Forward translocation of MTs in the cell body of an HGF-treated cell coinjected with rhodamine-labeled and C2CF-labeled tubulin. (a) The entire MT array at time 0 (just after photoactivation); (b and b′) the corresponding photoactivated region at the time, in minutes, indicated in the corner of each panel. (c) Plot of the position (in arbitrary units), over time, of the lamella, photoactivated MTs, and nucleus of the cell shown, emphasizing the discontinuous nature of cell movement: the lamella remains in place whereas the nucleus and MTs move forward. Bar, 10 μm.

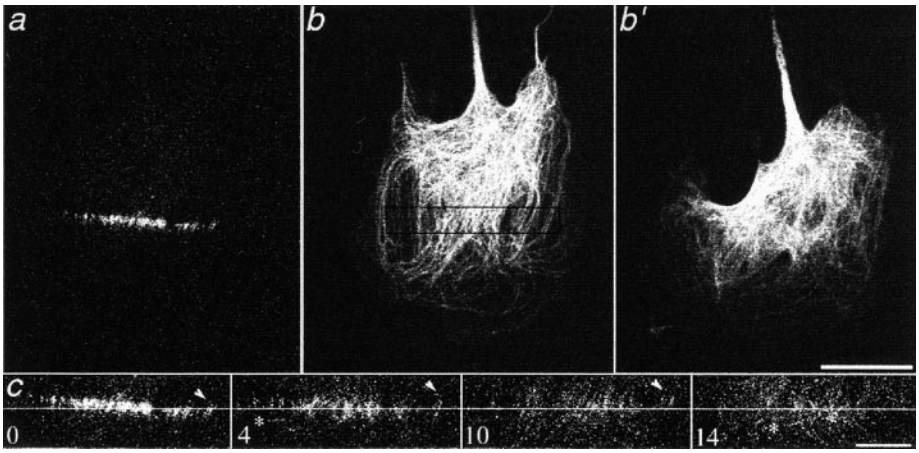

Figure 4. MTs in the transition zone of HGF-treated cells. Photoactivated MTs (a) and all MTs (b and b′) are shown in the larger panels; a and b are at 0 min after photoactivation, and b′ is at 16 min after photoactivation. Smaller panels (c) show a magnified view of the photoactivated MTs at the time shown (in minutes) after photoactivation. The box in b shows the relative location of the photoactivated MTs in a. Horizontal line is provided as a reference. Arrowheads in c indicate MTs which have moved rearward. Asterisks indicate MTs which have moved forward. (The direction of motility is toward the bottom of the page.) Many MTs remain stationary, as demonstrated by their position relative to the reference line. Bars: (a, b, and b′) 20 μm; (c) 10 μm.

cally occurs in sequential phases of lamellar extension, nuclear advancement, and tail retraction. For these experiments, photoactivation was typically performed during the phase of nuclear advancement (Fig. 3 c). As such, there was no correlation between the rate that the lamella extended and the rate of mark movement.

The Transition Zone of HGF-treated Cells Contains Stationary MTs

Thus far, the results demonstrate that photoactivated marks in the cell body move in the direction of cell motility, whereas those in the peripheral lamella move in the opposite direction, suggesting that MTs respond to the dominant local force. We tested this hypothesis by photoactivating MTs in the transition zone of HGF-treated cells (see Fig. 1 a). The results show that, in the transition zone, MTs are subject to both forward and rearward forces, and can be moved in both directions (Fig. 4 c). In addition, photoactivation in the transition zone always reveals some MTs that are not translocated, but are stationary with respect to the substrate. As shown in Fig. 4, stationary MTs are found in close proximity to MTs that are translocated. That adjacent MTs can be transported in different directions suggests that the forces responsible for their movement are highly local (Heidemann et al., 1999). One explanation for the presence of stationary MTs in the transition zone is that forward-directed forces from the cell body and rearward forces from the peripheral lamella meet, exerting no net force on a subset of MTs. In support of this possibility is the fact that stationary MTs can be induced to move by a local force, such as the advancing nucleus (see Fig. 3). Alternatively, stationary MTs may be tethered to the substrate in this region (Kaverina et al., 1998), which could explain why closely neighboring MTs are moved whereas the stationary ones are not.

MT Transport is Inhibited by BDM

Previous experiments have demonstrated that rearward MT movement in the peripheral lamella is actomyosin dependent (Waterman-Storer and Salmon, 1997), suggesting that actomyosin may contribute to MT movement in other cellular regions as well. To test this possibility, we first measured the behavior of photoactivated marks in the cell body of HGF-treated cells that did not locomote, as assessed by the lack of lamellar extension and nuclear advancement during the period of observation (compare Fig. 3 with Fig. 5). As shown in Fig. 5 a, MTs in the cell body of nonmoving cells did not undergo unidirectional transport, indicating that MT movement is correlated with translocation of the cell body, an actomyosin-dependent event (Svitkina et al., 1997). Note that although forward movement of the MTs is not observed in Fig. 5 a, the width of the photoactivated region increases in both directions over time.

As a second test to analyze the role of actomyosin in MT transport, we used the myosin inhibitor, BDM; as expected, lamellar extension was inhibited (Fig. 5 b). In addition, both unidirectional MT transport and cell body advancement ceased, confirming that these processes are indeed actomyosin driven (compare Fig. 5 with Fig. 3). BDM did not completely inhibit nuclear movement in 40% of HGF-treated cells, although the rate of nuclear movement in those cells was slowed considerably (average of 0.18 μm/min compared with 0.80 μm/min in non–BDM-treated cells). An additional mechanism for nuclear transport, such as has been shown for cytoplasmic dynein in other systems (Plamann et al., 1994; Xiang et al., 1994), could play a role.

In the transition zone of HGF-treated cells, BDM did not change the type of behavior we observed—that is, some MTs that were stationary and some MTs that underwent movement either forward or rearward; however, the distance that moved MTs traveled appeared to be somewhat reduced. Interestingly, BDM treatment also suppressed the extent of broadening of the photoactivated zone in the cell body (compare Fig. 5, a and b), indicating that myosin contributes to both unidirectional transport and bidirectional movement of MTs in interphase cells. The myosin inhibitor, ML7, produced similar results as BDM; however, cell rounding was more pronounced, making analysis more difficult. Detailed quantitative analysis of the role(s) of myosin II and other molecular motors in bidirectional MT

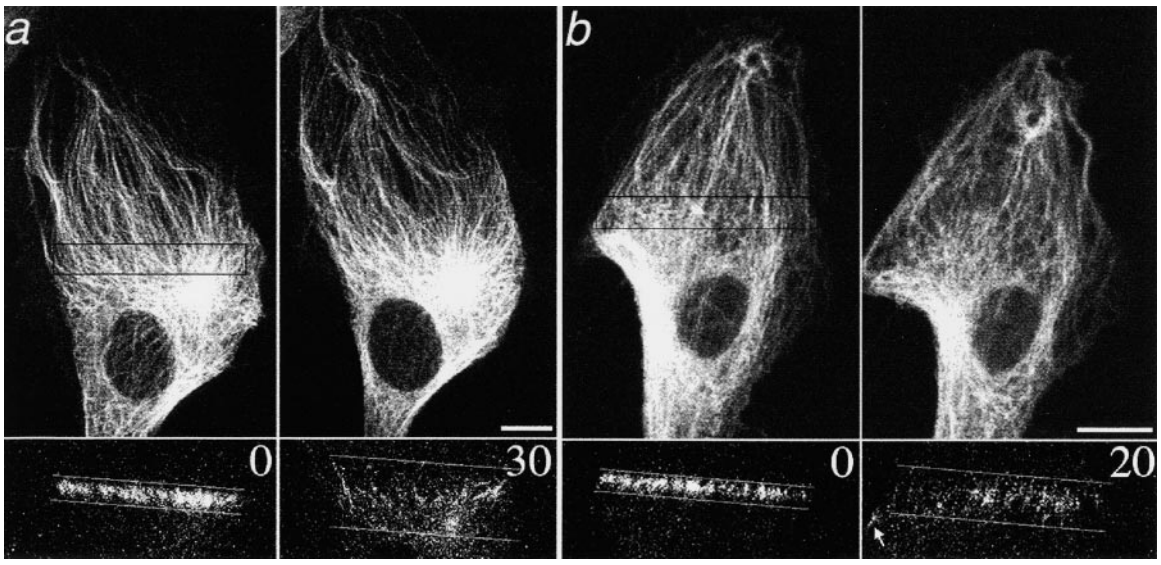

Figure 5. Photoactivation of a nonmotile HGF-treated cell (a) and an HGF-treated cell with 20 mM BDM (b). Top panels show the entire MT array; bottom panels show the photoactivated MTs. Boxes in the top panels show initial area of photoactivation; horizontal lines in the bottom panels are provided as a reference. Time after photoactivation is given in minutes in the corner of the lower panels. MTs do not move forward in the absence of cell motility; the nucleus and some MTs (arrow) shifted slightly rearward in b due to cell rounding as a result of BDM treatment. The leading edge is toward the top of the page for both cells. Bars, 10 μm.

movement will be reported elsewhere (Yvon, A.C., and P. Wadsworth, manuscript submitted for publication).

Forward Transport of MTs in the Retraction Tail of HGF-treated Cells

Photoactivated marks were made on the MTs in retraction tails to determine their dynamic properties and pattern of movement. Photoactivation was performed in a region that would allow observation of the marked MTs and the tip of the retraction tail in the same field of view. In all cases the mark moved toward the cell body; in no case was the mark stationary with respect to the substrate. In the cell shown in Fig. 6 a, the mark moved steadily toward the cell body over the period of observation. During the same period, tail retraction was steady for ~26 min then slowed (see Fig. 6 d), resulting in more distance between the mark and the tail's tip at the 40-min time point than at time 0 (Fig. 6 a).

The relationship between the rate of MT movement and the rate of tail movement was determined. Over the course of observation, tails typically experienced periods of steady retraction at a constant rate, as well as periods of slow, discontinuous movement (<0.1 μm/min); rates of tail and MT movement were calculated separately for these phases. As shown on the graph (e), the rates of MT and tail movement during periods of steady tail retraction are loosely correlated, but not tightly coupled. For the population of cells observed, the average rate of tail retraction during steady movement was 0.66 μm/min and the average rate of mark movement toward the cell body was 0.44 μm/min (n = 8). During discontinuous retraction (average rate = 0.07 μm/min), marked MTs moved slowly toward the cell body at an average rate of 0.13 μm/min (n = 7).

The MTs in a long tail must occupy less space when the tail retracts. In HGF-treated PtK cells, this is frequently accomplished by buckling of the MTs (Fig. 6 b), especially in tails that retract very quickly (Heidemann et al., 1999). Buckling can occur in the distal tail region (Fig. 6 b), or can extend into the cell body as the MTs approach it (Fig. 6 b′). Although the cell body was out of the field of view in these experiments, it must be relatively stationary or moving quite slowly for the approaching tail MTs to crumple into it. Buckled MTs have not been observed to break, as has been reported in other work (Waterman-Storer and Salmon, 1997), but it is not always possible to distinguish individual MTs in retraction tails.

Broadening of the Photoactivated Mark Is Independent of Cell Motility

An additional feature of MT behavior in HGF-treated cells is the increased width of the photoactivated mark over time. Mark broadening was observed in the retraction tail (Fig. 6 c), transition zone (see Fig. 4 c), and cell body of HGF-treated cells. Mark spreading was particularly clear in tails that retracted slowly (Fig. 6 c). The average increase in the width of the photoactivated mark was 45% in tails that retracted slowly or not at all, whereas the increase was only 21% in those that retracted steadily. This behavior is represented graphically in Fig. 6 d, which shows a plot of the tail movement and mark movement and broadening in a single cell over time. Although the tail is retracting steadily (0–26 min), the photoactivated mark maintains approximately the same width. Shortly after the tail pauses, the mark begins to broaden and continues to do so until the end of the observation period. The widening of the photoactivated zone must occur as individual fluorescent MTs move relative to one another.

As in the tails, faster, steady cell movement is generally correlated with less widening of the photoactivated zone (compare Fig. 3 a with Fig. 5 a). For example, the cell shown in Fig. 3 a was the fastest mover of any we observed and contained a photoactivated mark which underwent the least amount of spreading over the course of the ex-

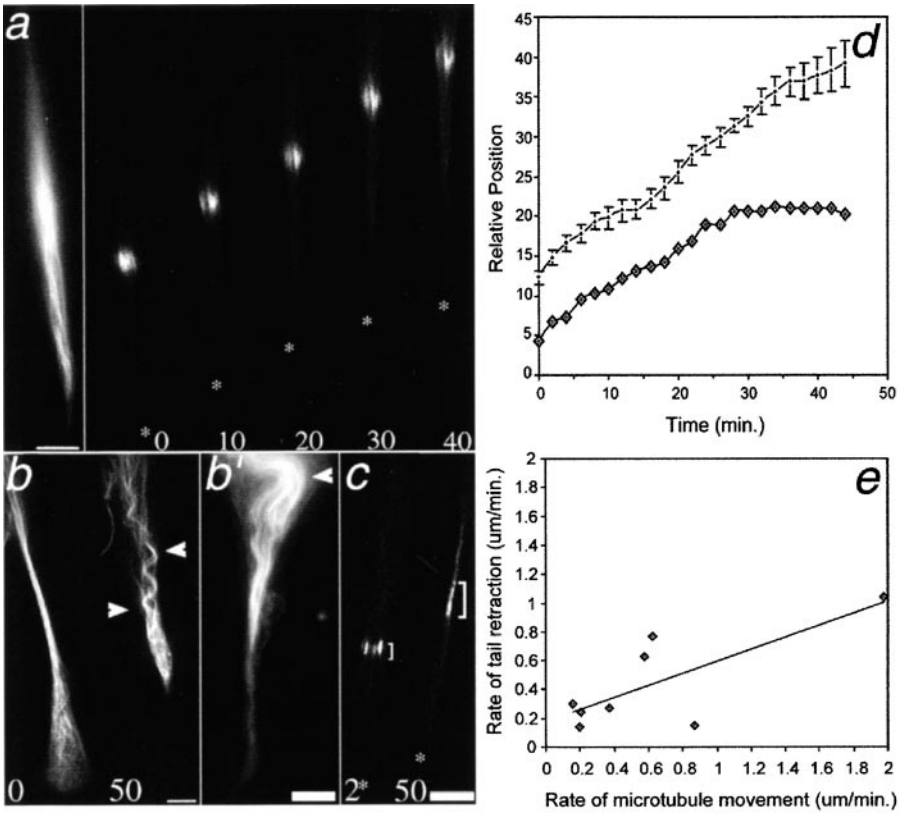

Figure 6. Photoactivated marks in the retraction tail of HGF-treated cells move toward the cell body, which is at the top of the page in a–c. (a) The mark in a steadily retracting tail moves steadily toward the cell body. The leftmost panel shows all MTs immediately after photoactivation; subsequent images show photoactivated MTs. (b) Rhodamine-labeled MTs in rapidly retracting tails buckle, indicated by arrowheads, as they are moved toward the cell body. Buckling of MTs can occur in distal (b) or proximal (b′) regions of the tail. Panels a and b′ represent the same cell; the field of view was moved toward the end of the sequence to image the junction of the tail and cell body. (c) The mark in a very slowly retracting tail widens as it is moved toward the cell body; only photoactivated MTs are shown. Brackets indicate the region measured for calculations of mark spreading. The brightness to the cell body side of the mark at 50 min is due to incorporation of photoactivated subunits; it is more apparent in this region because the MTs are very densely bundled. All times after photoactivation are given in minutes in the corner of each panel. Asterisks mark the tip of the retracting tails. (d) Graphical representation of cell shown in a and b′. The extent of widening of the photoactivated mark is inversely related to the rate of tail retraction. The position of the tip of the tail is indicated by diamonds. The position of the marked MTs and the relative width of the photoactivated mark are indicated by bars; the majority of mark widening occurs during a period of little or no tail retraction. (e) The rate of MT movement during eight periods of steady movement (see text) in seven retraction tails is loosely correlated with the rate of tail retraction during the same period. Bars, 5 μm.

periment. Note, however, that unlike the case in the retraction tail, the mark in nonmotile cells widens in both directions from its origin (see Fig. 5 a). Because this phenomenon can occur in the absence of cell motility, it must be independent of the unidirectional aspect of MT transport that is observed only in motile cells.

The Half Time for MT Turnover Is Decreased in HGF-treated Cells

The disparate persistence of the photoactivated marks in HGF-treated cells compared with control cells suggested that the turnover half time of the MT array might be different when motility is induced by HGF treatment. We measured the decay of fluorescence over time (see Materials and Methods); all marked MTs were included in the measurement, even if they had been transported from their initial location. To that end, note that MTs which are stable (i.e., not undergoing subunit exchange) are not necessarily stationary (i.e., not undergoing transport of the lattice).

The MT turnover half time in HGF-treated cells (6.2 min) was half that of untreated, control cells (11.8 min). Thus, treatment with HGF increases turnover, consistent with previous observations of MT plus end dynamic instability in MDCK cells (Wadsworth and Bottaro, 1996). Interestingly, the half time for MT turnover in the tails of HGF-treated cells was 11.7 min, nearly twice that of MTs in the lamellae of the same cells, directly demonstrating that MT behavior is regionally regulated.

Discussion

MT Transport Occurs in Response to Mechanical Forces

In these experiments, we have used photoactivation and photobleaching to mark the MT lattice in motile PtK2 cells. The results show that the majority of marks that persist on MTs in motile cells are transported in response to actomyosin-generated forces. The pattern of MT movement that we observe is consistent with studies mapping the forces of motile cells on the substrate (Galbraith and Sheetz, 1997; Pelham and Wang, 1999). Our results also indicate that the direction of transport depends on the location of the mark in the cell and not on MT polarity. Assuming that MTs are organized with their plus ends distal to the perinuclear region, forward-moving marked MTs in the cell body of HGF-treated cells are transported with their plus ends leading. If the same polarity is assumed for MTs in the retraction tail—plus ends distal—then MTs in this region are transported toward their minus ends. In both cases MTs move in the direction of cell motility.

MT Transport Is Distinct from MT Dynamics

In these experiments, we measured the behavior of the MT lattice in cellular regions where the behavior of MT ends could not be observed. However, overall MT turnover is increased in HGF-treated cells and experiments at their

periphery show that the plus ends of MTs are dynamic, undergoing tempered dynamic instability (Sammak et al., 1987; Wadsworth, 1999). Therefore, MT ends must be undergoing gain and loss of subunits, even as they are transported. In fact, previous studies have shown that the peripheral MT ends often undergo slow movements, as well as the rapid length changes characteristic of dynamic instability, and our observations now suggest that these slow movements may result from transport of the MT (Yvon and Wadsworth, 1997). In addition, it has been shown that the rearward, unidirectional transport of MTs in the periphery of motile cells does not require dynamic MTs (Waterman-Storer and Salmon, 1997), and low concentrations of drugs that block MT assembly and/or disassembly slow cell motility but do not halt it (Liao et al., 1995; Mikhailov and Gundersen, 1998). Therefore, we believe that MT transport is not dependent on MT dynamic behavior.

Although treadmilling, the equivalent net gain and loss of subunits at opposite polymer ends, could contribute to MT turnover, the MT transport that we observe is not due to treadmilling because a mark on a treadmilling MT remains stationary (Margolis et al., 1978; Rodionov and Borisy, 1997). The MT lattice is moved in the mitotic spindle by a process known as flux, whereby poleward movement of the MT lattice is coupled to coordinated plus end assembly and minus end disassembly (Mitchison and Sawin, 1990). This movement requires ATP and the kinesin-related protein, Eg5 (Mayer et al., 1999), and is likely to be mitosis specific. Therefore, we refer to the movement of the MT lattice that we observe as transport to distinguish it from flux.

Role of MT Dynamic Turnover in Cell Motility

Recent data suggest that MTs maintain cell polarity by regulating the cell's contact with the substrate (Kaverina et al., 1999). There is direct physical interaction between MTs and adhesion sites (Kaverina et al., 1998), leading to the hypothesis that relaxation signals are delivered, via MTs, to focal contacts in order to modulate the development of adhesions in a region-specific manner (Kaverina et al., 1999). In support of this hypothesis, their results show an eightfold increase in the frequency of contact targeting by MTs in the retracting versus the protruding regions of moving cells (Kaverina et al., 1999). Interestingly, our results show that MT turnover occurs at approximately half the rate in the retraction tail of HGF-treated cells as in the lamella, suggesting that more dynamic MTs at the front of the cell allow nascent focal contacts to mature, whereas more stable MTs at the rear of the cell target focal adhesions for disassembly.

What Is the Mechanism of MT Movement?

Photobleaching experiments on centrosomal MTs in nonmotile PtK cells showed that MTs that were released from the centrosome could be rapidly transported (8.9–40 μm/min), presumably with their plus ends leading (Keating et al., 1997). The rate and direction of transport suggest the involvement of a minus end–directed MT motor, such as cytoplasmic dynein or the kinesin-related protein ncd, both of which have been shown to move MTs in vitro (Vale et al., 1989; McDonald et al., 1990). Our data show that MT transport occurs at sites distant from the centrosome in motile cells; however, MT movement in HGF-treated cells is slow (0.1–1.2 μm/min); we did not observe fast MT transport. The rates of MT transport we observed were consistent with those of actomyosin-dependent events, such as locomotion of tissue culture cells and rearward movement of MTs in the peripheral lamella of newt lung epithelial cells (Svitkina et al., 1997; Waterman-Storer and Salmon, 1997), and considerably slower than those of MT motor-driven events.

Our work can also be compared with analogous marking experiments of the microfilament cytoskeleton. As is the case for MTs, microfilament behavior is also region specific in motile cells. In motile fish keratocytes, characterized by a large lamellipodium, marked microfilaments remain stationary with respect to the substrate as the cell moves over them, supporting the idea that actin's interaction with cell adhesion proteins generates the traction required for motility (Theriot and Mitchison, 1991). In locomoting heart fibroblasts, F-actin is moved rearward in the extreme cell periphery or lamellipodium by retrograde flow; in the lamella, actin filaments are stationary with respect to the substrate; in the cell body, one subset of F-actin moves forward at the rate of cell motility and another subset remains stationary (Cramer et al., 1997). The authors hypothesize that the stationary actin bundles form tracks against which myosin moves a subpopulation of F-actin to generate motile force.

Our results with BDM and in nonmoving cells strongly support the view that MT transport in motile HGF–treated cells is dependent on actomyosin contractility or F-actin movement. A potential mechanism for MT movement in HGF-treated cells is that MTs are directly or indirectly linked to the mobile F-actin populations in the cell periphery and cell body. The observation that many MTs are stationary in the transition zone could be a reflection of reduced actomyosin contractility in this region. In support of such a correlation, focal adhesions, presumable sites of traction (Theriot and Mitchison, 1991; Pelham and Wang, 1999), are disassembled as they approach the cell body region of migrating fibroblasts (Kaverina et al., 2000), a region analogous to the transition zone in HGF-treated cells. Alternatively, MTs in motile cells could be moved passively, as a result of cell locomotion, by virtue of the fact that they are contained within the elastic plasma membrane.

The observation that MT transport requires actomyosin forces is supported by results that have demonstrated that there is cross-talk between the actin and MT cytoskeletons (Waterman-Storer and Salmon, 1999; Waterman-Storer et al., 2000). For example, Waterman-Storer et al. (2000) recently showed that F-actin could move along stationary MTs in an in vitro system; the converse situation, in which MTs move along stationary actin filaments, seems equally likely. In addition, several recent studies have identified potential cross-linking molecules, such as myosin VI and DCLIP 170 (Lantz and Miller, 1998) and myosin V and kinesin (Huang et al., 1999), which may have a role in the direct interaction between MTs and F-actin. To that end, myosin V has been localized to MTs in *Xenopus* extracts, and may mediate a connection between the two cytoskeletal systems (Waterman-Storer et al., 2000). In addition to physical connections between actin and MTs, there may be signals that regulate their interactions as well. Waterman-

Storer and Salmon (1999) have also proposed a feedback model in which Rac1 activation by MT growth in the leading edge promotes further actin assembly in this region and RhoA activation by MT shortening in the cell body drives actomyosin contractility. This type of local activation of signaling molecules could also drive MT transport by regulating MT–microfilament interactions or by activating myosin.

Role of MT Transport in MT Organization and Cell Motility

Many MTs in interphase cells are noncentrosomal and there are several cell types with nonradial MT arrays, suggesting that there need to be alternate methods of organizing the MT cytoskeleton in addition to the centrosome (Vorobjev et al., 1997; Waterman-Storer and Salmon, 1997; Yvon and Wadsworth, 1997). MT transport could play a key role in MT organization by positioning MTs that were released from the centrosome (Keating et al., 1997) elsewhere in the cytoplasm, resulting in the establishment and maintenance of particular patterns of MT arrangement. In support of this model, several approaches show that some fraction of MTs is transported down the axon of neuronal cells, demonstrating that MT transport plays an essential role in the cytoskeletal organization of these asymmetric cells, although this is still a somewhat controversial issue (Baas and Brown, 1997). Conversely, transport of photoactivated MTs is not detected in fish melanophores (Rodionov et al., 1994), which maintain a radial, centrosomally focussed MT array, an organization that is likely to be essential for efficient pigment transport. MT transport might be especially important in cells with a noncentrosomal MT array. If the MTs are all focussed at the MT organizing center, the cell need only move the organizing center to move the array (Kupfer and Singer, 1989); however, if the array is noncentrosomal, it could either be disassembled and reassembled elsewhere (Yvon and Wadsworth, 1997), or the parts (i.e., MTs) could be transported individually. HGF-treated PtK cells contain a large number of noncentrosomal MTs (for review see Keating and Borisy, 1999), therefore movement of the array by repositioning the centrosome is not an effective method of relocating cytoplasmic MTs. Instead, these motile cells use MT transport to populate the advancing lamella with and deplete the retracting tail of MTs.

Conclusions

The results of the MT marking experiments presented here directly demonstrate that the MT lattice can be transported in motile cells, in addition to probing cellular space by elongation of MT ends. The direction of MT movement depends on the dominant actomyosin force in the region of the cell examined and may be influenced by the movement of F-actin subpopulations. In cells with numerous noncentrosomal MTs, transport is likely to play a significant and previously unrecognized role in MT organization and rearrangement.

We wish to thank Drs. Arshad Desai and Tim Mitchison for providing the caged C2CF probe and Dr. Aline Valster for assistance with tubulin preparation and labeling. We are also indebted to Mr. Dale Callaham for assistance with confocal microscopy; Mr. Vince VanBuren and Dr. Dave Gross for assistance with analysis of turnover data; and Ms. Mia Sorcinelli for assistance with analysis of the data. Drs. Lynne Cassimeris, Barbara Danowski, Clare Waterman-Storer, and Ted Salmon provided useful comments and critical evaluation of the manuscript. We would also like to acknowledge the thoughtful comments of the reviewers, whose suggestions helped to greatly improve the manuscript.

This project was supported by National Science Foundation grant MCB-9723273.

Submitted: 9 May 2000
Revised: 6 October 2000
Accepted: 9 October 2000

References

Baas, P.W., and A. Brown. 1997. Slow axonal transport: the polymer transport model. *Trends Cell Biol.* 7:380–384.

Cramer, L.P., M. Siebert, and T.J. Mitchison. 1997. Identification of novel graded polarity actin filament bundles in locomoting heart fibroblasts: implications for the generation of motile force. *J. Cell Biol.* 136:1287–1305.

Danowski, B. 1989. Fibroblast contractility and actin organization are stimulated by microtubule inhibitors. *J. Cell Sci.* 93:255–266.

Desai, A., and T.J. Mitchinson. 1998. Preparation and characterization of caged fluorescein tubulin. *Methods Enzymol.* 298:128–1320.

Euteneuer, U., and M. Schliwa. 1984. Persistent, directional motility of cells and cytoplasmic fragments in the absence of microtubules. *Nature*. 310:58–61.

Galbraith, C.G., and M.P. Sheetz. 1997. A micromachined device provides a new bend on fibroblast traction forces. *Proc. Natl. Acad. Sci. USA*. 94:9114–9118.

Gundersen, G.G., and J.C. Bulinski. 1988. Selective stabilization of microtubules oriented toward the direction of cell migration. *Proc. Natl. Acad. Sci. USA*. 85:5946–5950.

Harris, A.K. 1994. Locomotion of tissue culture cells considered in relation to ameboid locomotion. *Int. Rev. Cytol.* 150:35–68.

Heidemann, S.R., S. Kaech, R.E. Buxbaum, and A. Matus. 1999. Direct observations of the mechanical behaviors of the cytoskeleton in living fibroblasts. *J. Cell Biol.* 145:109–122.

Huang, J.D., S.T. Brady, B.W. Richards, D. Stenolen, J.H. Resau, N.G. Copeland, and N.A. Jenkins. 1999. Direct interaction of microtubule- and actin-based transport motors. *Nature*. 397:267–270.

Kaverina, I., K. Rottner, and J.V. Small. 1998. Targeting, capture, and stabilization of microtubules at focal adhesions. *J. Cell Biol.* 142:181–190.

Kaverina, I., O. Krylyshkina, and J.V. Small. 1999. Microtubule targeting of substrate contacts promotes their relaxation and dissociation. *J. Cell Biol.* 146:1033–1044.

Kaverina, I., O. Krylyshkina, M. Gimona, K. Beningo, Y. Wang, and J.V. Small. 2000. Enforced polarisation and locomotion of fibroblasts lacking microtubules. *Curr. Biol.* 10:739–742.

Keating, T.J., and G.G. Borisy. 1999. Centrosomal and non-centrosomal microtubules. *Biol. Cell*. 91:321–329.

Keating, T.J., J.G. Peloquin, V.I. Rodionov, D. Momcilovic, and G.G. Borisy. 1997. Microtubule release from the centrosome. *Proc. Natl. Acad. Sci. USA*. 94:5078–5083.

Kupfer, A., and S.J. Singer. 1989. Cell biology of cytotoxic and helper T cell functions: immunofluorescence microscopy of single cells and cell couples. *Annu. Rev. Immunol.* 7:309–337.

Lantz, V.A., and K.G. Miller. 1998. A class VI unconventional myosin is associated with a homologue of a microtubule-binding protein, cytoplasmic linker protein-170, in neurons and at the posterior pole of *Drosophila* embryos. *J. Cell Biol.* 140:897–910.

Liao, G., T. Nagasaki, and G.G. Gundersen. 1995. Low concentrations of nocodazole interfere with fibroblast locomotion without significantly affecting microtubule level: implications for the role of dynamic microtubules in cell locomotion. *J. Cell Sci.* 108:3473–3483.

Lin, C.-H., and P. Forscher. 1993. Cytoskeletal remodeling during growth cone–target interactions. *J. Cell Biol.* 121:1369–1383.

Margolis, R.L., L. Wilson, and B.I. Kiefer. 1978. Mitotic mechanism based on intrinsic microtubule behavior. *Nature*. 272:450–452.

Mayer, T.U., T.M. Kapoor, S.J. Haggarty, R.W. King, S.L. Schreiber, and T.J. Mitchison. 1999. Small molecule inhibitor of mitotic spindle bipolarity identified in a phenotype-based screen. *Science*. 286:971–974.

McDonald, H.B., R.J. Stewart, and L.S.B. Goldstein. 1990. The kinesin-like *ncd* protein of *Drosophila* is a minus end-directed microtubule motor. *Cell*. 63: 1159–1165.

Mikhailov, A., and G.G. Gundersen. 1998. Relationship between microtubule dynamics and lamellipodium formation revealed by direct imaging of microtubules in cells treated with nocodazole or taxol. *Cell Motil. Cytoskeleton*. 41:325–340.

Mitchison, T.J., and L.P. Cramer. 1996. Actin-based cell motility and cell locomotion. *Cell*. 84:371–379.

Mitchison, T.J., and M.W. Kirschner. 1984. Dynamic instability of microtubule growth. *Nature*. 312:237–242.

Mitchison, T.J., and K.E. Sawin. 1990. Tubulin flux in the mitotic spindle: where does it come from, where is it going? *Cell Motil. Cytoskeleton.* 16:93–98.

Pelham, R.J., and Y.-l. Wang. 1999. High resolution detection of mechanical forces exerted by locomoting fibroblasts on the substrate. *Mol. Biol. Cell*. 10: 935–945.

Plamann, M., P.F. Minke, J.H. Tinsley, and K.S. Bruno. 1994. Cytoplasmic dynein and actin-related protein Arp1 are required for normal nuclear distribution in filamentous fungi. *J. Cell Biol.* 127:139–149.

Rodionov, V.I., and G.G. Borisy. 1997. Microtubule treadmilling *in vivo*. *Science*. 275:215–218.

Rodionov, V.I., S.-S. Lim, V.I. Gelfand, and G.G. Borisy. 1994. Microtubule dynamics in fish melanophores. *J. Cell Biol.* 126:1455–1464.

Sammak, P.J., G.J. Gorbsky, and G.G. Borisy. 1987. Microtubule dynamics in vivo: a test of mechanisms of turnover. *J. Cell Biol.* 104:395–405.

Sloboda, R.D., W.L. Dentler, and J.L. Rosenbaum. 1976. Microtubule associated proteins and the stimulation of tubulin assembly *in vitro*. *Biochemistry*. 15:4497–4505.

Stoker, M., E. Gherardi, M. Perryman, and J. Gray. 1987. Scatter factor is a fibroblast-derived modulator of epithelial cell mobility. *Nature*. 327:239–242.

Svitkina, T.M., A.B. Verhovsky, K.M. McQuade, and G.G. Borisy. 1997. Analysis of the actin–myosin II system in fish epidermal keratocytes: mechanism of cell body translocation. *J. Cell Biol.* 139:397–415.

Tanaka, E., T. Ho, and M. Kirschner. 1995. The role of microtubule dynamics in growth cone motility and axonal growth. *J. Cell Biol.* 128:139–155.

Theriot, J.A., and T.J. Mitchison. 1991. Actin microfilament dynamics in locomoting cells. *Nature*. 352:126–131.

Vale, R.D., D.R. Soll, and I.R. Gibbons. 1989. One-dimensional diffusion of microtubules bound to flagellar dynein. *Cell*. 59:915–925.

Vasiliev, J.M. 1991. Polarization of pseudopodial activities: cytoskeletal mechanisms. *J. Cell Sci.* 98:1–4.

Vorobjev, I.A., T.M. Svitkina, and G.G. Borisy. 1997. Cytoplasmic assembly of microtubules in cultured cells. *J. Cell Sci.* 110:2635–2645.

Wadsworth, P. 1999. Regional regulation of microtubule dynamics in polarized, motile cells. *Cell Motil. Cytoskeleton.* 42:48–59.

Wadsworth, P., and D. Bottaro. 1996. Microtubule dynamic turnover is suppressed during polarization and stimulated in HGF scattered MDCK epithelial cells. *Cell Motil. Cytoskeleton.* 35:225–236.

Waterman-Storer, C.M., and E.D. Salmon. 1997. Actomyosin-based retrograde flow of microtubules in the lamella of migrating epithelial cells influences microtubule dynamic instability, induces microtubule breakage and generates noncentrosomal microtubules. *J. Cell Biol.* 139:417–434.

Waterman-Storer, C.M., and E.D. Salmon. 1999. Positive feedback interactions between microtubule and actin dynamics during cell motility. *Curr. Opin. Cell Biol.* 11:61–67.

Waterman-Storer, C.M., J.W. Sanger, and J.M. Sanger. 1993. Dynamics of organelles in the mitotic spindles of living cells: membrane and microtubule interactions. *Cell Motil. Cytoskeleton*. 26:19–39.

Waterman-Storer, C.M., R.A. Worthylake, B.P. Liu, K. Burridge, and E.D. Salmon. 1999. Microtubule growth activates Rac1 to promote lamellipodial protrusion in fibroblasts. *Nat. Cell Biol.* 1:45–50.

Waterman-Storer, C., D.Y. Duey, K.L. Weber, J. Keech, R.E. Cheney, E.D. Salmon, and W.M. Bement. 2000. Microtubules remodel actomyosin networks in *Xenopus* egg extracts via two mechanisms of F-actin transport. *J Cell Biol.* 150:361–376.

Xiang, X., S.M. Beckwith, and N.R. Morris. 1994. Cytoplasmic dynein and actin-related protein Arp1 are required for normal nuclear distribution in filamentous fungi. *J. Cell Biol.* 127:139–149.

Yvon, A.C., and P. Wadsworth. 1997. Non-centrosomal microtubule formation and measurement of minus end microtubule dynamics in A498 cells. *J. Cell Sci.* 110:2391–2401.